

Dual phase-amplitude silicon modulator driven by an ENZ transparent conducting oxide

Juan Navarro-Arenas^{1,2}, Jorge Parra², Pablo Sanchis^{2,*}

¹Institute of Materials Science (ICMUV), Universitat de València, Carrer del Catedratic José Beltrán Martínez, 2, 46980, Valencia, Spain

²Nanophotonics Technology Center, Universitat Politècnica de València, Camino de Vera s/n, 46022, Valencia, Spain

*pabsanki@ntc.upv.es

An ultracompact electro-optical ENZ/Si modulator with dual phase-amplitude operation is proposed. A 4 μm -long modulator is designed to achieve a π -phase shift modulation or an amplitude modulation with an extinction ratio of 10 dB.

Keywords: ENZ, TCO, electro-optical, modulator

INTRODUCTION

Nanoelectronics technology has always relied on the continued scaling down of the transistor size to achieve the exponential growth in computing speed seen during the last decades. Today, however, the limits of lithography, the frontier with quantum phenomena—in which transistors may not continue to function as intended—, and the huge costs of fabrication, address the need to start planning for the end of Moore's Law [1]. In this context, silicon photonics (SiPh) has demonstrated many advantages such as ultra-high speed, ultra-low energy consumption and new functionalities. In the case of neuromorphic computing, for example, recently demonstrated optical neural networks offer computation speeds that are orders of magnitude beyond von Neuman electronic computers [2]. Other emerging industries that could benefit from SiPh are LiDAR systems [3] or integrated quantum computing based on photonics [4].

For most of the applications, optical phase shifters and amplitude modulators are required to perform operations with light. Furthermore, simultaneous phase and amplitude modulation would be very valuable in many cases. Optical neural networks require complex-valued modulation to shape the inputs and outputs of the network [5], [6]. This is usually achieved through a concatenation of an asymmetric Mach–Zehnder interferometer (MZI), with one arm being phase-modulated, followed by a phase shifter. Tuning principles are varied in the current literature; e.g. those based on the thermo-optic effect [7], on the free-carrier effect [8], or the micro-electro-mechanical systems (MEMS) [9]. However, trade-offs in terms of speed, power consumption and footprint are usually given.

In this paper, an ultracompact dual phase shifter-amplitude modulator is proposed. The tuning mechanism relies on the epsilon-near-zero (ENZ) effect in transparent conducting oxides (TCOs) of high mobility. The ENZ occurs when the real permittivity becomes close to zero resulting in a large enhancement of modal confinement and extreme optical nonlinear effects [10]. In our device such an effect can be triggered electro-optically with a metal-oxide-semiconductor (MOS) stack structure mounted on top of a Si waveguide. Such a compact implementation eliminates the need to build two sets of modulators—one for phase, one for amplitude—and, therefore, significantly reduces the device footprint.

Description of device operation

TCO's permittivity in the near-infrared regime can be well described by the interaction of light with free electrons. Following Drude's model, possible switching mechanisms can either manipulate the effective electron mass m_e^* or the electronic concentration N —the plasma frequency is proportional to the square root of N/m_e^* —. Usually, effective electron mass is perturbed all-optically by intraband transitions triggered upon the absorption of high-power pulses [10],[11], while concentration can be tuned electro-optically by means of a metal/oxide/TCO capacitor structure [12].

Here an electro-optical modulator is implemented in a silicon waveguide loaded with a metal/oxide/TCO layer stack (see Fig. 1(a)). The TCO acts as a semiconductor in the proposed device. It is modeled as a high-mobility cadmium oxide (the parameters and equations of our model can be found in literature [10-12]). The TCO acts also as the ground electrode of the device. The top metal layer serves as a second

electrode while the insulator (SiO_2) behaves as a charge blocking layer. When a gate voltage is applied (V_G) in the capacitor, electrons accumulate at the interface between the insulator and the TCO. Obtaining the electron density distribution inside the TCO requires solving the biased Poisson's equation to evaluate the band bending. To this end, the Thomas-Fermi approximation (MTFA), developed by Paasch and Übensee [12] was implemented and solved numerically by the finite element method (FEM).

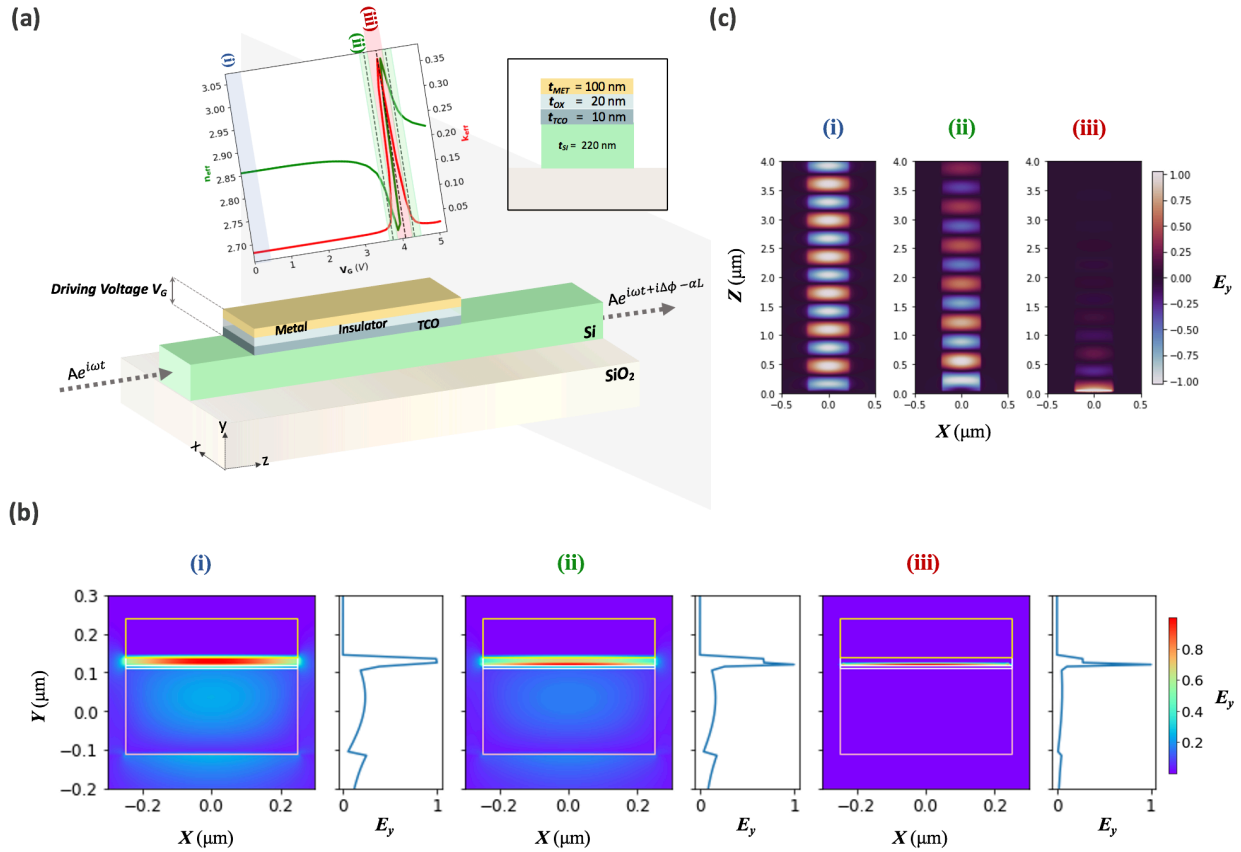


Fig. 1. (a) Sketch of the dual phase-amplitude modulator. The silicon waveguide is loaded by a capacitor stack (Au/ SiO_2 /TCO) that drives the modulator performance so that the effective index of the propagating optical mode is changed when a gate voltage is applied. E_y field distribution cross-section in the (b) Z-X (inside the TCO layer) and (c) in the Y-X plane (including a 1D cross-section at $x = 0 \mu\text{m}$) of the device in the (i) OFF, (ii) phase and (iii) amplitude operation regimes.

The solution gives rise to a relationship between the Drude's permittivity and the applied gate voltage. This relationship is used to calculate the optical mode of the hybrid silicon waveguide loaded by the capacitor structure and its complex effective refractive index (n_{eff} and κ_{eff}). The optical mode was calculated by the FEM method implemented in the RSoft CAD environment from Synopsys. For an optimized device geometry such as the one presented in the cross-section of the device, the resulting effective index variation (see both insets in Fig. 1(a)) defines three regimes in which the device can operate: (i) OFF state, in which the modulator has low optical losses and the transmission is maximized (blue region in Fig. 1), (ii) phase modulation, in which the effective refractive index is tuned past or just after the ENZ resonance (green regions) so that a net phase difference is extracted with minimal losses, (iii) amplitude modulation, in which the index is tuned at the midpoint of the ENZ resonance (red region) so that the modal confinement is maximized in the low permittivity region and, thus, optical absorption is maximized.

Guided modes, accompanied by its cross-section at $x = 0 \mu\text{m}$, for the three operation regimes are shown in Figure 1b. Confinement within the TCO's accumulation layer is enhanced the most in the amplitude operation regime, as can be seen in Figure 1b(iii). In the phase regime, Figure 1b(ii), a large portion of the E_y field exist within oxide film. On the contrary, Figure 1b(i) shows that the modal overlap with the TCO's accumulation layer is minimal.

Dual phase-amplitude modulator performance

The modulator was designed for operation at a wavelength of 1550 nm and TM polarization. The 3D spatial distribution of the mode propagation was computed by the finite-difference time-domain method (3D-FDTD) for the three configurations. In the OFF state, which is shown in Fig. 1c(i), i.e. without applying a voltage to the modulator, the insertion losses are as low as 0.1 dB/ μm . In the phase modulation operation regime, which is depicted in Figure 1c(ii), the device is driven by a voltage of 3.7 V, inducing a $0.24\pi/\mu\text{m}$ phase shift with optical losses around 0.75 dB/ μm . Finally, in the amplitude modulation operation regime shown in Figure 1c(iii), the device requires a voltage of 4V for which an extinction ratio of 2.2 dB/ μm is achieved. Therefore, a modulation length of around 4 μm is necessary to obtain a π -phase shift with insertion losses of 3 dB. For such a modulation length, the optical losses at the OFF state are as low as 0.4 dB while an extinction ratio of around 10 dB is achieved when switching to the amplitude modulation regime. Another important aspect is the energy consumption, as it grows quadratically with the gate voltage and scales proportionally with the footprint of the device. In the proposed modulator, a 4- μm long device would require an energy below 500 fJ for modulation.

Conclusions

Phase-amplitude modulation functions are mostly accomplished by means of a concatenation of Mach–Zehnder interferometers or ring resonator structures and individual phase shifter in current photonic integration circuits. These approaches come at expense of a large device footprint that could limit large-scale integration. To the best of our knowledge, the proposed ENZ/Si modulator is the first one of its class to present the possibility of manipulating the phase or the amplitude of the optical field with high performance in a compact (few microns long) device. Therefore, such a device would be highly beneficial for emerging high-impact fields as neural networks or reconfigurable photonics.

Acknowledgements

This work was supported by grants PID2019-111460GB-I00, Margarita Salas fellowship (MS21-037) funded by the European Union Next-Generation EU, funded by MCIN/AEI/10.13039/501100011033, by "ERDF A way of making Europe" and "ESF Investing in your future", PROMETEO/2019/123 by Generalitat Valenciana, and 2-PAID-10-22 by Universitat Politècnica de València.

References

- [1] M. Haselman and S. Hauck, *The Future of Integrated Circuits: A Survey of Nanoelectronics*, in Proc. IEEE, vol. 98, no. 1, pp. 11–38, 2010.
- [2] Y. Shen et al., *Deep learning with coherent nanophotonic circuits*, Nat. Photonics, vol. 11, no. 7, pp. 441–446, 2017.
- [3] X. Zhang, K. Kwon, J. Henriksson, J. Luo, and M. C. Wu, *A large-scale microelectromechanical-systems-based silicon photonics LiDAR*, Nature, vol. 603, no. 7900, pp. 253–258, 2022.
- [4] J. W. Silverstone et al., *On-chip quantum interference between silicon photon-pair sources*, Nat. Photonics, vol. 8, no. 2, pp. 104–108, 2014.
- [5] R. Wang et al., *Multicore Photonic Complex-Valued Neural Network with Transformation Layer*, Photonics, vol. 9, no. 6, 2022.
- [6] H. Zhang et al., *An optical neural chip for implementing complex-valued neural network*, Nat. Commun., vol. 12, no. 1, p. 457, 2021.
- [7] J. Parra et al., *Silicon thermo-optic phase shifters: a review of configurations and optimization strategies*, in preparation.
- [8] X. Chen et al., *Modeling and Analysis of Optical Modulators Based on Free-Carrier Plasma Dispersion Effect*, IEEE Trans. Comput. Des. Integr. Circuits Syst., vol. 39, no. 5, pp. 977–990, 2020.
- [9] C. Errando-Herranz, A. Y. Takabayashi, P. Edinger, H. Sattari, K. B. Gylfason, and N. Quack, *MEMS for Photonic Integrated Circuits*, IEEE J. Sel. Top. Quantum Electron., vol. 26, no. 2, pp. 1–16, 2020.
- [10] E. Li and A. X. Wang, *Femto-Joule All-Optical Switching Using Epsilon-Near-Zero High-Mobility Conductive Oxide*, IEEE J. Sel. Top. Quantum Electron., vol. 27, no. 2, pp. 1–9, 2021.
- [11] J. Navarro-Arenas, J. Parra, and P. Sanchis, *Ultrafast all-optical phase switching enabled by epsilon-near-zero materials in silicon*, Opt. Express 30, 14518, 2022.
- [12] X. Liu et al., *Tuning of Plasmons in Transparent Conductive Oxides by Carrier Accumulation*, ACS Photonics, vol. 5, no. 4, pp. 1493–1498, Apr. 2018.